

Available online at www.sciencedirect.com**ScienceDirect**

Procedia Engineering 90 (2014) 308 – 313

**Procedia
Engineering**www.elsevier.com/locate/procedia

10th International Conference on Mechanical Engineering, ICME 2013

Numerical Study on Aerodynamic Drag Reduction of Racing Cars

S.M. Rakibul Hassan*, Toukir Islam, Mohammad Ali, Md. Quamrul Islam

Department of Mechanical Engineering, Bangladesh University of Engineering and Technology, Dhaka-1000, Bangladesh

Abstract

Aerodynamic drag is one of the main obstacles to accelerate a solid body when it moves in the air. When a racing car or road vehicle burns fuel to accelerate, drag force pulls it from back to reduce the speed and hence the fuel efficiency is adversely affected. About 50 to 60% of total fuel energy is lost only to overcome this adverse aerodynamic force. To win a race, which may be decided by fraction of second, the racing cars need a faster acceleration, which is possible by reducing the drag force by optimizing its shape to ensure stream-lining or reducing the separation. Reduction of aerodynamic drag has become one of the prime concerns in vehicle aerodynamics. This article is concentrated on different aspects analysis of aerodynamic drag of racing cars and different drag reduction techniques such as rear under body modification and exhaust gas redirection towards the rear separation zones. Through a numerical process (Finite Volume Method) of solving the Favre-averaged Navier-Stokes equations backed by k -epsilon turbulence model, the drag coefficient of the car under analysis is found to be 0.3233 and it is evident that the drag can be reduced up to 22.13% by different rear under-body modifications and up to 9.5% by exhaust gas redirection towards the separated region at the rear of the car. It is also evident that if somehow the negative pressure area and its intensity at the rear of the car can be minimized, the separation pressure drag is subsequently reduced.

© 2014 The Authors. Published by Elsevier Ltd. This is an open access article under the CC BY-NC-ND license (<http://creativecommons.org/licenses/by-nc-nd/3.0/>).

Selection and peer-review under responsibility of the Department of Mechanical Engineering, Bangladesh University of Engineering and Technology (BUET)

Key Words: Aerodynamic drag; separation; coefficient of drag; under-body diffuser; exhausts gas redirection.

1. Introduction

Aerodynamic drag of racing cars has probably received highest attention over last five decades in experimental and practical field of fluid dynamics. Many researchers and authors have described different forms of

* Corresponding author. Tel.: +8801920795748
E-mail address: rakibulhassan21@gmail.com

drag, possible reasons behind them and several ways of minimizing the drag. Katz's [1] work was fully devoted for the racing car aerodynamics and he described the different aspect of car design or streamlining starting from the first generation automobiles to most recent models, but no numerical or experimental procedure was explained to measure the drag. Computational analysis to reduce the drag is performed by Barbut et al. [2], Rouméas et al. [3] on road vehicle and by Guilmineau [4] on the simplified car body (Ahmed body). Islam and Mamun [5] performed numerical and experimental study to measure the aerodynamic drag, but their work was concentrated on sedan car only and they did not investigated any drag reduction technique. Aerodynamics of sedan cars and racing cars are different in many aspects like speed and effects of body constructions. Koike et al. [6] introduced vortex generators to reduce the drag of racing cars. But effectiveness of vortex generator is restricted by the body shape of the car. Work of Krishnani [7] is not only very informative about the sport utility car, but also for drag reduction techniques. But this work does not concern with racing cars specifically. Adem [8] worked on vehicle aerodynamics and described the aspects of aerodynamic drag, but his work was subjected to a pick-up truck. Work of Damjanović et al. [9] is one of the recent studies on race car aerodynamic drag that includes both two dimensional and three dimensional analyses. But they only described the reduction of drag by using spoiler. Islam et al. [10] worked on calculating the drag force of racing car. A comparative drag analysis of sedan and square back car is performed by Bijlani et al. [11] and found that sedan car produces less drag than square-back car. A very few research paper has clear indication about the specific area that has to be used in drag calculation as different drag force is subjected to different area. In this work, numerical simulations are performed to analyse the drag of a racing car and some procedures to reduce it by reducing the flow separation.

2. Numerical Method

Favre-averaged Navier-Stokes equations are used here, where time-averaged effects of the flow turbulence on the flow parameters are considered. Flow simulation employs transport equations for the turbulent kinetic energy and its dissipation rate, the so-called k-ε model. Flow simulation employs one system of equations to describe both laminar and turbulent flows and transition from a laminar to turbulent state or vice versa is possible. The set of equations for Newtonian fluids are:

$$\frac{\partial(\rho u_i)}{\partial x_i} = 0$$

$$\frac{\partial(\rho u_i u_j)}{\partial x_j} + \frac{\partial P}{\partial x_i} = \frac{\partial}{\partial x_i} \left(\mu \left(\frac{\partial u_i}{\partial x_j} + \frac{\partial u_j}{\partial x_i} - \frac{2}{3} \delta_{ij} \frac{\partial u_k}{\partial x_k} \right) + \mu_t \left(\frac{\partial u_i}{\partial x_j} + \frac{\partial u_j}{\partial x_i} - \frac{2}{3} \delta_{ij} \frac{\partial u_k}{\partial x_k} \right) - \frac{2}{3} \rho k \delta_{ij} \right) - \rho g_i$$

$$\frac{\partial(\rho u_i H)}{\partial x_i} = \frac{\partial}{\partial x_i} \left[u_j \left(\mu \left(\frac{\partial u_i}{\partial x_j} + \frac{\partial u_j}{\partial x_i} - \frac{2}{3} \delta_{ij} \frac{\partial u_k}{\partial x_k} \right) + \mu_t \left(\frac{\partial u_i}{\partial x_j} + \frac{\partial u_j}{\partial x_i} - \frac{2}{3} \delta_{ij} \frac{\partial u_k}{\partial x_k} \right) - \frac{2}{3} \rho k \delta_{ij} \right) \right] - \rho g_i u_i - \mu_t \left(\frac{\partial u_i}{\partial x_j} + \frac{\partial u_j}{\partial x_i} - \frac{2}{3} \delta_{ij} \frac{\partial u_k}{\partial x_k} \right) - \frac{2}{3} \rho k \delta_{ij} \frac{\partial u_i}{\partial x_i} + \rho \varepsilon$$

$$H = h + \frac{u^2}{2}$$

Here δ_{ij} is the Kronecker delta, h is the thermal enthalpy, μ is the dynamic viscosity coefficient, μ_t is the turbulent eddy viscosity coefficient and k is the turbulent kinetic energy. Point to be noted that both k and μ_t are zero for laminar flow. In the frame of k-ε turbulence model, $\mu_t = f_\mu \frac{C_\mu \rho k^2}{\varepsilon}$. Here f_μ is the turbulent viscosity factor; defined as,

$$f_\mu = [1 - \exp(-0.025 R_y)]^4 \times [1 + \frac{y^2}{z_0^2}]^{-1} \quad \text{where, } R_T = \text{ and } R_y = \frac{\rho u^2 y}{\mu}$$

Here y is the distance from the wall. This function of f_μ allows us to take into account laminar-turbulent transition. Two additional transport equations are used to describe the turbulent kinetic energy and dissipation at steady state,

$$\frac{\partial}{\partial x_j} (\rho u_i k) = \frac{\partial}{\partial x_i} \left[\left(\mu + \frac{\mu_t}{\sigma_k} \right) \frac{\partial k}{\partial x_i} \right] + \tau_{ij}^R \times \frac{\partial u_i}{\partial x_j} - \rho \epsilon + \mu_t P_B$$

$$\frac{\partial}{\partial x_j} (\rho u_i \epsilon) = \frac{\partial}{\partial x_i} \left[\left(\mu + \frac{\mu_t}{\sigma_\epsilon} \right) \frac{\partial \epsilon}{\partial x_i} \right] + C_{\epsilon 1} \frac{\epsilon}{k} \left[f_1 \times \tau_{ij}^R \times \frac{\partial u_i}{\partial x_j} + \mu_t C_B P_B \right] - C_{\epsilon 2} f_2 \frac{\rho \epsilon^2}{k}$$

Here, $f_1 = 1 + \left(\frac{0.05}{f_\mu} \right)^2$, $f_2 = 1 - \exp(-R_T^{-2})$, $P_B = -\frac{g_i}{\sigma_B} \times \frac{1}{\rho} \frac{\partial p}{\partial x_i}$

Now for these equations σ_k is unity when $P_B > 0$ and zero otherwise. $\sigma_B = 1$, $C_\mu = 0.09$, $C_{\epsilon 1} = 1.44$, $C_{\epsilon 2} = 1.92$, $\sigma_\epsilon = 1.3$. These values are found empirically. These equations describe both laminar and turbulent flow. The cell-centred finite volume (FV) method is used to obtain conservative approximations of the governing equations on the locally refined rectangular mesh. The governing equations are integrated over a control volume which is a grid cell, and then approximated with the cell-centred values of the basic variables. The integral conservation laws may be represented in the form of the cell volume and surface integral equation:

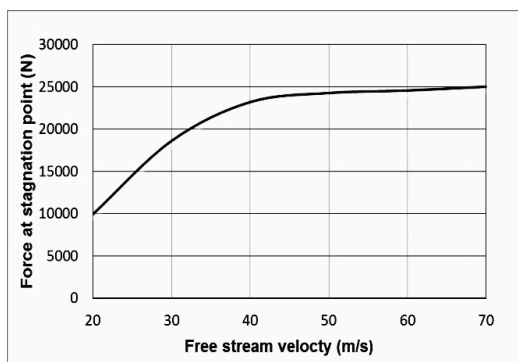
$$\frac{\partial}{\partial t} \int U dv + \oint F \cdot ds = \int Q dv$$

are replaced by the discrete form $\frac{\partial}{\partial t} (Uv) + \sum_{cell\ faces} F \cdot s = Qv$. The second-order upwind approximations of fluxes F are based on the implicitly treated modified Leonard's QUICK approximations [12] and the Total Variation Diminishing (TVD) method [13]. The size of computational domain is (length×height×width) 17.85295626 m × 3.988927894 m × 6.01184566m. Length of the car is 4.434m and the gap between the road and the car = 0.10702837178m. Number of grid used in computation is 109,543.

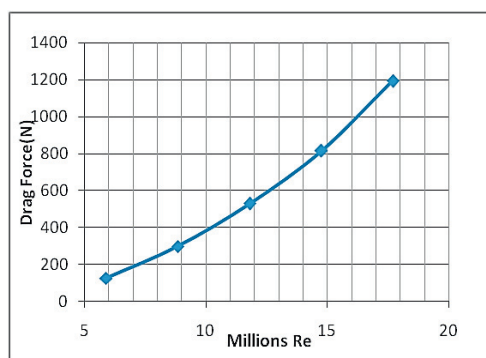
3. Result and Discussion

3.1. Effect of Velocity on Drag Force

Drag force is the result of the pressure difference between the front and the rear of the car. As the velocity of car increases, the stagnation pressure increases as shown in Fig. 1(a) and at the same time the pressure at rear decreases too due to the increase in momentum of air. So the difference between the pressure at stagnation or front and the pressure at rear of the car increases as the velocity and hence Reynolds no. increases. The relation between the drag force and Reynolds no. is as Fig.1(b). At the free stream velocity 50 m/s, the coefficient of drag C_D is found to be 0.3233. Further analysis for drag reductions are done regarding this as a base value and compared the relative reduction of drag.



(a)



(b)

Fig. 1. (a) Force at stagnation points for different free stream velocity. (b) Drag force at different Reynolds Number.

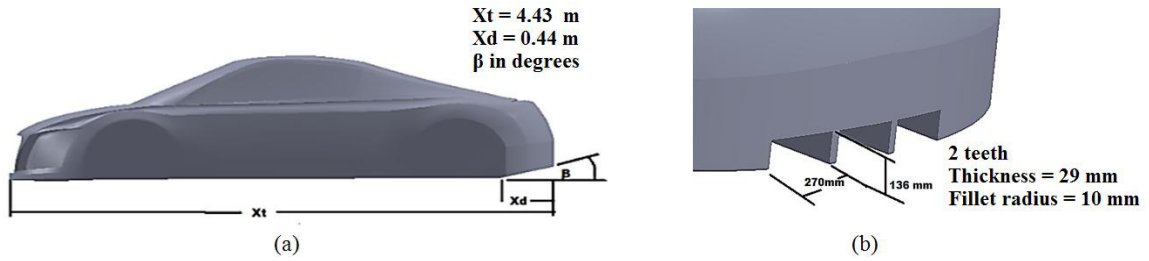


Fig. 2. (a) Rear under-body slicing at angle β degree. (b) Rear body diffuser

3.2. Drag Reduction

3.2.1. Rear Underbody Modification

When a car moves forward, a low pressure zone is created behind the car. This low pressure zone pulls the car from behind opposite to its moving direction and creates pressure drag. This low pressure zone is created due to the separation of flow and consequent vortices are generated at the back of the car. To reduce this pulling-back effect, a unique idea is to slice the rear under-body at certain angles as shown in Fig. 2(a) which actually directs some flow from the under-body to the low pressure zone. This reduces the effect of vortices and low pressure effect. Another popular way to reduce the rear end separation is to use under-body diffuser as shown in Fig. 2(b) which also adds elegance in aesthetics of the car, but it has less flow area as the rear under-body is not fully sliced out. So less reduction of drag is experienced then similar degree of rear under-body slicing. In Fig.3 a pressure cut plot for base of the car at 50 m/s free steam velocity shows a certain envelope of pressure range of 100800 Pa to 102000 Pa. Another small envelope inside this envelop for $\beta=0$, shows further pressure reduction in the ranges of 100700 Pa to 100799 Pa. With the increase of slicing angle β , the low pressure area decreases and the coefficient of drag decreases too.

Table 1. For rear under-body modification, drag reduction at flow velocity 50 m/s

modifications	Descriptions of modifications	C_D	ΔC_D	% of reduction of C_D
None	-	0.3233	-	-
Modification1	$\beta = 2.5^\circ$, rear under-body sliced	0.3083	0.01500	4.639
Modification2	$\beta = 5.0^\circ$, rear under-body sliced	0.2962	0.02707	8.373
Modification3	$\beta = 10.0^\circ$, rear under-body sliced	0.2694	0.05386	16.58
Modification4	$\beta = 12.5^\circ$, rear under-body sliced	0.2517	0.07156	22.13
Modification5	$\beta = 12.5^\circ$, under-body diffuser	0.2926	0.03070	9.5

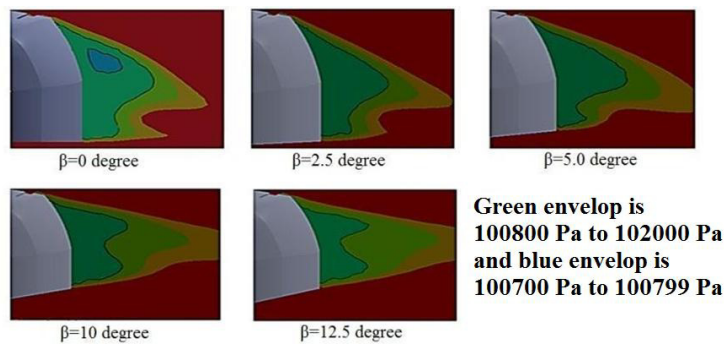


Fig.3. Pressure contour at the rear end (base) of car at different β , showing reduction of low pressure zone (green) with increasing β .

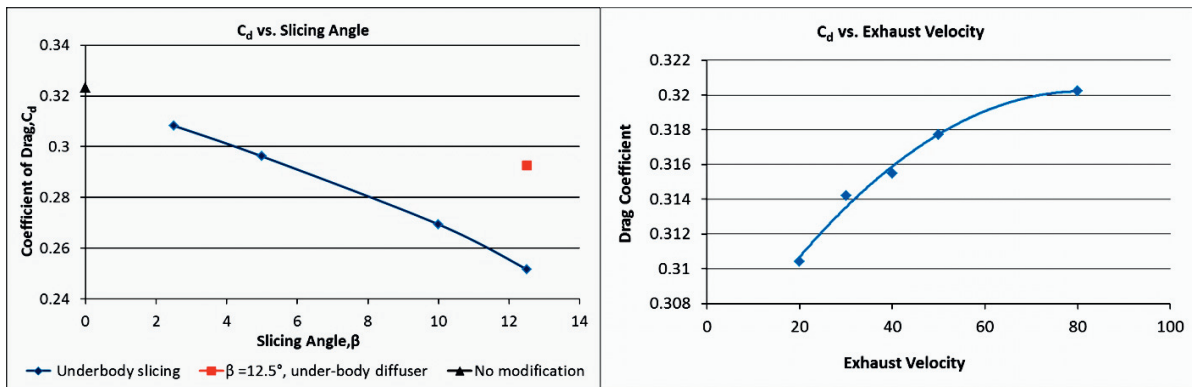


Fig. 4. Change in C_d due to different modification.

Fig. 5. Change in C_d with exhaust gas velocity

As the slicing angle increases in case of under body slicing, more air is permitted to flow to the low pressure region. As a result the size of low pressure zone is reduced as shown in Fig. 3 which indicates the increase in pressure at that region. So normal force along x axis i.e. the drag force decreases and hence the C_d decreases too. From Fig.4 it can be seen that C_d decreases almost linearly with the increase in slicing angle. For under body diffuser, though the drag force decreases, the reduction is not as high as that for same degree of under body slicing. The difference is shown for $\beta = 12.5^\circ$ in Fig. 4.

3.2.2. Exhaust Gas Redirection

Another way of reducing drag is using the exhaust gas to fill the low pressure zone behind the car. The exhaust gas can be flown from the exhaust pipe outlet at different speed. The flow is directed towards the low pressure zone behind the car so that it can reduce the negative pressure i.e. increase the pressure to reduce drag force.

Table 2: Change in C_d with exhaust gas velocity.

Item	No mod.	Mod. 1	Mod. 2	Mod. 3	Mod. 4	Mod. 5
Exhaust Velocity(m/s)	-	80	50	40	30	20
C_d	0.3200	0.3202	0.3177	0.3155	0.3142	0.3104

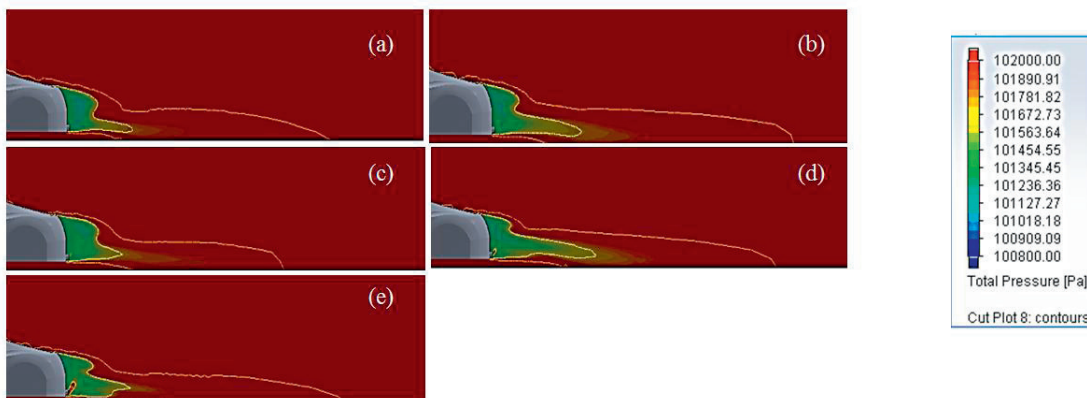


Fig.6. Pressure contour at the rear of the car at exhaust velocity (a) 20m/s (b) 30 m/s (c) 40 m/s (d) 50 m/s (e) 80 m/s

Though the reduction in drag is very small as observed in table 2, in case of racing car this ‘very small’ drag reduction can be decisive between the winner and loser. The exhaust gas is the combination of carbon dioxide, steam, and Nitrogen. Concentrations of these gasses are used in simulation according to their volumetric fraction in case of stoichiometric reaction. Pressure, Temperature and angle of emission of exhaust gas that have been used in simulation are 2atm, 300⁰C and 45⁰ respectively.

Here in Fig. 5 it can be seen that the value of coefficient of drag decreases as the speed of exhaust gas decreases. Reason behind this is at higher velocity, exhaust gas induce the surrounding air to create a lower pressure, which elongate or enlarge the low pressure zone or reduce the pressure again and increase the drag. This can be seen from the pressure contour in Fig. 6.

4. Conclusion

Flow separation is responsible for the major portion of aerodynamic drag of racing cars. The aerodynamic drag coefficient of the car model used here is found to be 0.3233. The main design consideration to reduce the drag of any bluff should be- keep the flow attached to the body as much as possible. That means maintaining streamline shape, reducing surface roughness, fewer joints of the body or avoiding sharp fillets, controlling lift force, air or exhaust gas flow towards the low pressure zone at the rear portion of the car etc. These must be considered while designing a car for higher speed and acceleration as well as for better fuel efficiency and control. Aerodynamic drag reduction by rear under body modification results in up to 22.13% and rear under-body diffuser results 9.5% reduction of drag coefficient. Exhaust gas redirecting towards the low pressure zone at the rear of the car is proved to be effective to some extent, which paves the way of future improvement for future researchers. About 3.3% drag coefficient can be reduced by this procedure considering the ideal exhaust gas composition.

References

- [1] Joseph Katz, Race Car Aerodynamics- Designing for Speed, first ed., Bently Publishers, 1995.
- [2] Dan Barbut, Eugen Mihai Negrus, CFD analysis for road vehicles - case study, Incas Bulletin, 3(2011) 15-22.
- [3] M. Rouméas, P. Gilliéron and A. Kourta, Drag Reduction by Flow Separation Control on a Car after Body, International Journal for Numerical Methods in Fluids, 60(2009) 1222–1240.
- [4] Emmanuel Guilmineau, Computational Study of Flow around a Simplified Car Body, Journal of Wind Engineering and Industrial Aerodynamics, 96(2008) 1207–1217.
- [5] Md. MunirIslam, M.Mamun, Computational Drag Analysis over a Car Body, International Conference on Marine Technology, Dhaka, Bangladesh, 2010.
- [6] MasaruKoike, TsunehisaNagayoshiandNaokiHamamoto, Research on Aerodynamic Drag Reduction by Vortex Generator, Mitsubishi Motors Technical Reviews, 16(2004) 13-18.
- [7] PramodNariKrishnani, CFD study of drag reduction of a generic sport utility vehicle, Thesis for M.Sc. Mechanical Engineering, California State University, Sacramento, 2009.
- [8] Feysal AhmedAdem, Drag Reduction of Pickup Truck Using Add-on Devices, Thesis for M.Sc. in Mechanical Engineering, California State University, Sacramento, 2009.
- [9] DarkoDamjanović, DražanKozak, MarijaŽivić, ŽeljkoIvandić, TomislavBaškarić, CFD analysis of concept car in order to improve aerodynamics, JärműipariInnováció, University of Osijek, Croatia, 2011.
- [10] Toukir Islam, S.M. Rakibul Hassan and Dr. M. Ali, Aerodynamic Drag of Racing Cars, Global Engineering, Science and Technology Conference, Dhaka, Bangladesh, 2012
- [11] BhaviniBijlani, Dr. Pravin P. Rathod, Prof. Arvind S. Sorthiya, Experimental and Computational Drag Analysis of Sedan and Square-Back Car, International Journal of Advanced Engineering Technology, 4(2013) 63-65.
- [12] P.J. Roache, Technical Reference of Computational Fluid Dynamics, Hermosa Publishers, Albuquerque, New Mexico, 1998.
- [13] C. Hirsch, Numerical computation of internal and external flows, John Wiley and Sons, Chichester, England, 1988.